

Electronic Supporting Information

Intercepting a Transient Non-Hemic Pyridine N-Oxide Fe(III) Species

Nhat Tam Vo, Christian Herrero, Régis Guillot, Tanya Inceoglu, Winfried Leibl, Martin Clémancey, Patrick Dubourdeaux, Geneviève Blondin, Ally Aukauloo* and Marie Sircoglou*

I.	Materials and Instrumentation	2
II.	Experimental procedures.....	2
III.	Crystal structure determination	4
IV.	Catalysis	6
V.	UV-visible Absorption spectroscopy	8
VI.	EPR spectroscopy	9
VII.	Mössbauer spectroscopy	10
VIII.	Mass spectrometry	11
IX.	Infra-Red spectroscopy	12
X.	Reactivity with NaClO	13
XI.	DFT Calculations.....	16

I. Materials and Instrumentation

Iron(III) chloride hexahydrate (98%) and iodosylbenzene diacetate (98 %) were purchased from Sigma-Aldrich. Sodium hypochlorite solution (5 %) was purchased from Acros Organics. Water-¹⁸O (97%) was purchased from Euriso-Top. The ⁵⁷Fe-enriched metal (95.55%) was obtained from Chemgas (SAS JLD Instruments).

UV-visible absorption spectra were recorded on a Varian Cary 60 UV-vis spectrophotometer using 1 cm quartz cuvettes.

X-band EPR spectra were recorded on a Bruker ELEXSYS 500 spectrometer equipped with a Bruker ER 4116DM X-band resonator, an Oxford Instrument continuous flow ESR 900 cryostat, and an Oxford ITC 503 temperature control system. Sample of typically 1 mM of complexes and intermediates were prepared in acetonitrile added with 0.1 M TBAPF₆ then transferred to a degassed EPR tube and frozen to 77 K before their analysis.

Electrospray ionization mass spectrometry experiments were recorded on a Thermo Scientific DSQ 2004 model under either positive or negative modes. Samples were prepared as a 100–200 μM solution in acetonitrile and were directly injected into the spectrometer. For the detection of intermediate species, the samples were frozen in liquid nitrogen following their preparation and melt to room temperature just prior to injection in the spectrometer.

The high-performance gas chromatography experiments (HPGC) were performed on a GC-2010 system from Shimadzu with a Zebron ZB Semi-Volatiles column (25 m, 0.25 mm, 0.25 mm). The Shimadzu GC software was used to perform and analyze chromatograms.

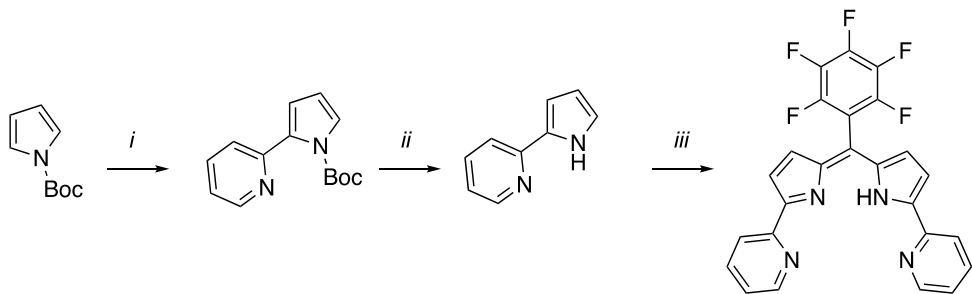
Mössbauer spectra were recorded at 4.2 and 5.8 K, either on a low field Mössbauer spectrometer equipped with a Janis SVT-400 cryostat or on a strong-field Mössbauer spectrometer equipped with an Oxford Instruments Spectromag 4000 cryostat containing an 8 T split-pair superconducting magnet. Both spectrometers were operated in a constant acceleration mode in transmission geometry. The isomer shifts are referenced against that of a room-temperature metallic iron foil. Analysis of the data was performed with a home-made program.

Infra-red spectra were recorded on an attenuated total reflectance-infrared (ATR-IR) Thermo-Nicole t 6700 FTIR spectrometer, equipped with a mercury-cadmium-telluride (MCT) detector. 5 μL of the sample solution (1 mM) was deposited onto the diamond prism of the ATR-IR and the solvent was evaporated under a stream of nitrogen gas until a dry film was formed. For each spectrum, 200 sample scans were recorded with a resolution of 4 cm⁻¹, a speed of 1.8988 kHz and an aperture of 10 mm from 4000 cm⁻¹ to 500 cm⁻¹.

X-ray diffraction data were collected using a VENTURE PHOTON100 CMOS Bruker diffractometer with Micro-focus IuS source Mo Kα radiation for crystal grown in ACN/Et₂O and Cu Kα radiation for crystal grown in acetone. Crystals were mounted on a CryoLoop (Hampton Research) with Paratone-N (Hampton Research) as cryoprotectant and then flash-frozen in a nitrogen-gas stream at 100 K. The temperature of the crystal was maintained at the selected temperature by means of an N-Helix cooling device to within an accuracy of ±1K. The data were corrected for Lorentz polarization and absorption effects. The structures were solved by direct methods using SHELXS-97¹ and refined against F² by full-matrix least-squares techniques using SHELXL-2018² with anisotropic displacement parameters for all non-hydrogen atoms. Hydrogen atoms were located on a difference Fourier map and introduced into the calculations as a riding model with isotropic thermal parameters. All calculations were performed by using the Crystal Structure crystallographic software package WINGX.³

II. Experimental procedures

The **DPPyH** ligand was synthesized in 3 steps by optimizing a previously reported⁴ procedure.



i) 2-bromopyridine (2.26 mL, 23.60 mmol, 1 equiv.) was dissolved in a 2:1:1 mixture of dioxane, ethanol and water (200 mL). This solution was degassed under argon for 1 h. [Pd(PPh₃)₄] (2.73 g, 2.36 mmol, 0.1 equiv.) and (N- Boc-2-pyrrolyl)boronic acid (5.00 g, 23.6 mmol, 1 equiv.) were then added. The mixture was stirred for 20 min. K₂CO₃ (10.00 g, 0.24 mol, 10 equiv.) was added, and the reactional mixture was stirred vigorously at 107 °C for 2 h. After cooling to room temperature, solvents were evaporated. The obtained solid was dissolved in 200 mL of ethyl acetate then washed with 200 mL of aq. K₂CO₃ 1M (3 times). The organic phase was dried over Na₂SO₄ then filtered and concentrated. The residue was purified by column chromatography on silica gel (petroleum ether/ethyl acetate, 9:1) to yield 2-(N-Boc-1H-pyrrol-2-yl)pyridine as a yellow oil (3.9 g, 68%). ¹H NMR (CDCl₃, 250 MHz): δ = 1.36 (s, 9 H, CH₃), 6.25 (t, J = 3.3 Hz, 1 H), 6.42 (dd, J = 3.3, 1.8 Hz, 1 H), 7.20 (ddd, J = 12, 4.8, 1.2 Hz, 1 H), 7.36–7.43 (m, 2 H), 7.68 (td, J = 7.5, 1.8 Hz, 1 H), 8.60–8.64 (m, 1 H) ppm.

ii) 2-(N-Boc-1H-pyrrol-2-yl)pyridine (3.9 g, 16.05 mmol) was dissolved in CH₂Cl₂ (30 mL) and aq. HCl 3 M (30 mL) was added. The biphasic mixture was vigorously stirred at room temperature for 60 h. The solution was neutralized by addition of a sat. aq. NaHCO₃ solution and extracted with 100 mL of water (3 times). The organic phase was dried over Na₂SO₄ and filtered. The solution was concentrated to yield 2-(2-Pyrrolyl)pyridine as a white solid (2.28 g, 95 %). ¹H NMR (CDCl₃, 360 MHz): δ = 6.30 (dt, J = 2.6, 3.6 Hz, 1 H), 6.7 (m, 1 H), 6.9 (m, 2 H), 7.03 (dd, J = 2.0, 5.5 Hz, 1 H), 7.54 (d, J = 7.7 Hz, 2 H), 7.62 (td, J = 7.7, 1.6 Hz, 1 H), 8.45 (d, J = 5 Hz, 1 H), 9.8 (br. s, NH) ppm.

iii) *p*-toluenesulfonic acid (4.5 g, 23.7 mmol, 3 equiv.) was dissolved in toluene (50 mL). The Dean stark method was used to eliminate water in the solution. 2-(2-Pyrrolyl)pyridine (2.28 g, 15.8 mmol, 2 equiv.), pentafluorobenzaldehyde (1.55 g, 7.9 mmol, 1 equiv.) and 1,1,2,2- tetrachloroethane (50 mL) were then added. The mixture was heated at 138 °C under argon for 7 day, after which it was basified with aq. K₂CO₃ (1 M). The aqueous phase was extracted with chloroform, and the combined organic phases were concentrated and dissolved in dichloromethane (100 mL). A solution of 2,3-dichloro-5,6-dicyano-1,4-benzoquinone (10.5 g, 47.4 mmol, 6 equiv.) in tetrahydrofuran (80 mL) was then added dropwise. The reactional mixture was stirred overnight at room temperature. The solvents were evaporated. The obtained solid was dissolved in 200 mL chloroform, then extracted 3 times with 200 mL K₂CO₃ 1 M. The organic phase was dried with Na₂SO₄ and filtered then concentrated. Precipitation in methanol (30 mL) at -20 °C followed by filtration and drying allowed the isolation of the DPPyH ligand (2 g, 54 %) as a brown solid .¹H NMR (CDCl₃, 250 MHz): δ = 6.59 (d, J = 4.4 Hz, 2 H, H_{pyrrol}), 7.10 (d, J = 4.4 Hz, 2 H, H_{pyrrol}), 7.29 (m, 2 H), 7.82 (dd, J = 7.8, 1.6 Hz, 2 H), 8.20 (d, J = 8.1 Hz, 2 H), 8.72 (d, J = 4.7 Hz, 2 H), 13.70 (br. s, 1 H, NH) ppm.

[FeDPPyCl₂]: A solution of DPPy ligand (100 mg, 215 μmol, 1 equiv.) in methanol (20 mL) was added dropwise to a solution of FeCl₃·6H₂O (58.3 mg, 215 μmol, 1 equiv.) in methanol (10 mL) at room temperature, followed by addition of diethyl ether (50 mL) in order to precipitate the solid. The brown residue was filtered and dried under vacuum to give complex [FeDPPyCl₂] (116 mg, 197 μmol, 91%). Single crystals were obtained by slowly diffusing diethyl ether to a saturated solution of complex [FeDPPyCl₂] in acetonitrile. ESI⁺-HRMS: calcd. For [C₂₅H₁₂ClF₅FeN₄]⁺ 554.0015; found 553.9995. UV-vis (CH₃CN): 668 nm (ϵ = 10 000 M⁻¹cm⁻¹), 589 nm (ϵ = 21 600 M⁻¹cm⁻¹), 320 nm (ϵ = 27 200 M⁻¹cm⁻¹), 298 nm (ϵ = 27 700 M⁻¹cm⁻¹).

Iodosylbenzene⁵ (PhIO): 30 mL of 3 M sodium hydroxide was added over a 5 min period into iodosylbenzene diacetate (5 g., 15.5 mmol) placed in a 50 mL flask with vigorous stirring. The reaction mixture was stirred for

an additional 45 minutes to complete the reaction. The solid was filtered and washed 3 times with 100 mL water then with 50 mL chloroform (3 times). The obtained solid was dried under vacuum to yield 2.9 g PhIO (85 %).

$^{57}\text{FeCl}_3$: The ^{57}Fe -enriched FeCl_3 was synthesized according to the literature.⁶ ^{57}Fe -enriched iron powder (100 mg) was suspended in ethanol (30 mL) and HCl was bubbled through the reaction mixture for 3 hours. The solvent was then removed by rotary evaporation and placed under high vacuum for 12 h.

$^{57}[\text{FeDPPyCl}_2]$: The ^{57}Fe -enriched complex was prepared by metalation with the ^{57}Fe -enriched FeCl_3 using the procedure described above.

Stoichiometric oxidation of $[\text{FeDPPyCl}_2]$ by PhIO: Solid PhIO (10eq., 1.1 mg) was added to a solution of the $[\text{Fe}(\text{DPPy})\text{Cl}_2]$ complex (10 mL, 50 μM) at room temperature. The reaction mixture was sonicated for 10 s, then the insoluble PhIO was filtered off using a syringe filter. Alternatively, a freshly prepared solution of PhIO in MeOH (1 eq., 3 μL , 50 mM) was added to the solution of the $[\text{FeDPPyCl}_2]$ complex (3 mL, 50 μM). A slightly lesser conversion was observed in that case (see Fig S6). For labelling experiment, the 1st procedure was performed on a 1mL volume scale, followed by the addition of 20 μL of ^{18}O -labeled water.

III. Crystal structure determination

CCDC 1966063-1966064 contains the supplementary crystallographic data for this paper. These data can be obtained free of charge from the Cambridge Crystallographic Data Centre via <http://www.ccdc.cam.ac.uk/Community/Requestastructure>.

3 Structures were obtained by X-ray analysis of single crystals grown form $\text{Et}_2\text{O}/\text{ACN}$ at rt (A), acetone at 30°C (B,C). Their main features are summed up below, and crystallographic details are given in what follows. According to a CCDC search, we found that the average Fe(III)-N bond length in Fe(III) porphyrin complexes is 2.02 Å. While, the average length for Fe(III)-pyridine bonds is 2.15 Å with only 10% of reported structures showing bond distances over 2.23 Å.

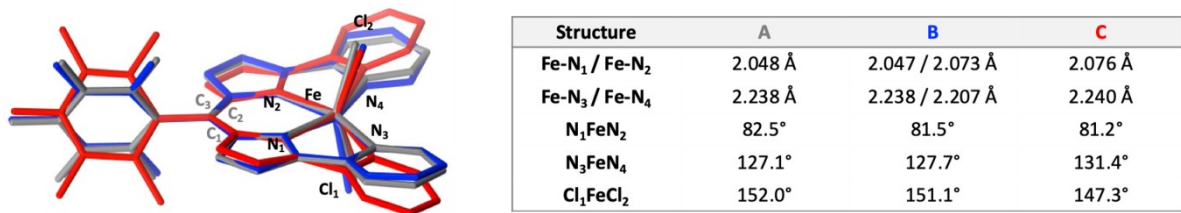


Figure S1: Left : Overlay along $\text{N}_1\text{-C}_1\text{-C}_2\text{-C}_3\text{-N}_2$ fragment of the FeDPPy in A, B, C (right, H and C_6F_5 omitted); Right : Selected parameters showing 1st coordination sphere distortions along the 3 forms.

- a. Structure obtained from crystals grown in ACN/ Et_2O (A)

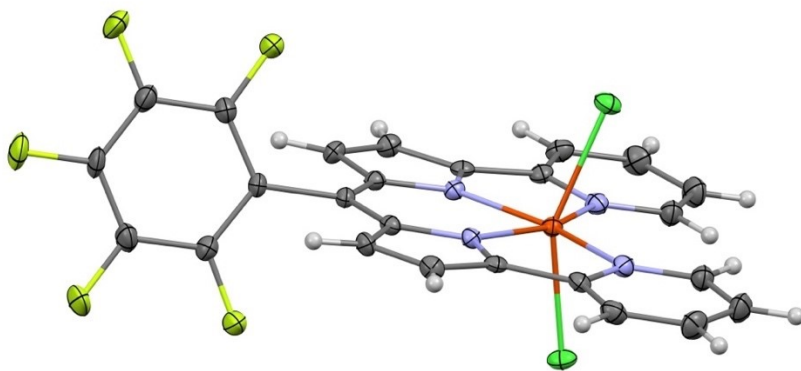


Figure S2: ORTEP representation at 30% of probability of X-Ray structure of $[FeDPPyCl_2]$ complex.

The presence of solvent molecules could easily be seen by residual peaks located in closed spherical cavities (Figure S3).

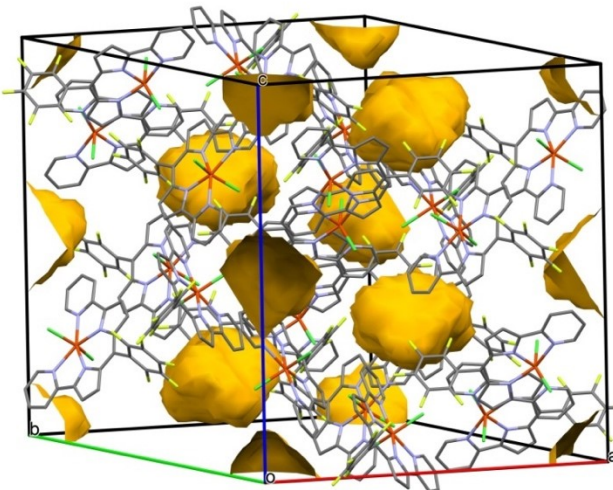


Figure S3: Crystal packing displaying space occupied by solvent molecules.

Unfortunately, they were disordered so badly that it could not be modeled even with restraints. Consequently, SQUEEZE³ (from PLATON) was used to calculate the void space, the electron count and to get a new HKL file. According to the SQUEEZE results and the different experimental evidence, a total number 14 CH₃CN solvent molecules (308 electrons) were considered per unit cell. Without solvent molecules: R1= 0.0848 for 3835 reflections of I > 2σ(I) and wR2= 0.2502 for all data. With solvent molecules (SQUEEZE): R1= 0.0784 for 3835 reflections of I > 2σ(I) and wR2= 0.1902 for all data, the volume fraction was calculated to 1203 Å³ which corresponds to 11% of the unit cell volume, and to 305 electrons per unit cell allocated to solvent molecules. The crystal data collection and refinement parameters are given in Table S1.

b. Structures obtained from crystals grown in acetone at 30°C (B and C)

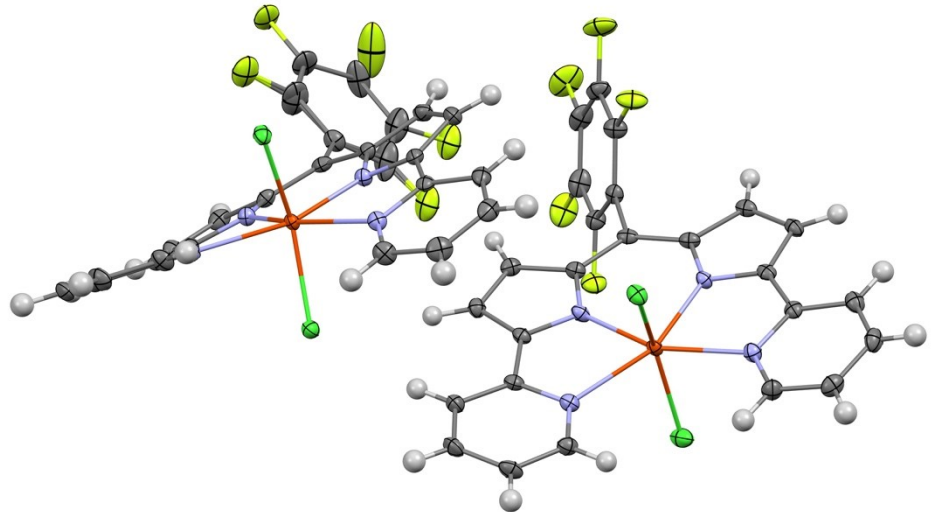


Figure S4: ORTEP representation at 30 % of probability of X-Ray structure of the two crystallographically independent molecules of [FeDPPyCl₂] complex.

In the crystal of the [FeDPPyCl₂] complex, the asymmetric unit is composed of one and a half molecules. One of [FeDPPyCl₂] complexes is situated on two-fold symmetry axes. The crystal data collection and refinement parameters are given in Table S2.

Table S1: Crystallographic data and structure refinement details from crystals grown in ACN/Et₂O.

Compound	[FeDPPyCl ₂] (A)
Empirical Formula	C ₂₅ H ₁₂ Cl ₂ F ₅ FeN ₄ [+ 7/9 (C ₂ H ₃ N)]
M _r	590.14
Crystal size, mm ³	0.08 x 0.08 x 0.04
Crystal system	trigonal
Space group	R -3 c
a, Å	22.4084(16)
b, Å	22.4084(16)
c, Å	25.9110(19)
α, °	90
β, °	90
γ, °	120
Cell volume, Å ³	11267.7(18)
Z ; Z'	18; 1/2
T, K	100 (1)
Radiation type ; wavelength Å	MoKα; 0.71073
F ₀₀₀	5310
μ, mm ⁻¹	0.868
θ range, °	2.623–30.530
Reflection collected	100 553
Reflections unique	3 835
R _{int}	0.1980
GOF	1.023
Refl. Obs. (I>2σ(I))	2 070
Parameters	170
wR ₂ (all data)	0.1902
R value (I>2σ(I))	0.0784
Largest diff. peak and hole (e-.Å ⁻³)	0.901; -0.511

Table S2: Crystallographic data and structure refinement details from crystals grown in acetone at 30°C.

Compound	[FeDPPyCl ₂] (B,C)
Empirical Formula	C ₂₅ H ₁₂ Cl ₂ F ₅ FeN ₄
M _r	590.14
Crystal size, mm ³	0.26 x 0.10 x 0.05
Crystal system	monoclinic
Space group	C 2/c
a, Å	19.907(3)
b, Å	13.511(2)
c, Å	26.718(5)
α, °	90
β, °	104.497(8)
γ, °	90
Cell volume, Å ³	6957(2)
Z ; Z'	12 ; 3/2
T, K	100 (1)
Radiation type ; wavelength Å	CuKα; 1.54178
F ₀₀₀	3540
μ, mm ⁻¹	7.755
θ range, °	3.417 – 66.749
Reflection collected	52 122
Reflections unique	6 155
R _{int}	0.0422
GOF	1.021
Refl. Obs. (I>2σ(I))	5 818
Parameters	512
wR ₂ (all data)	0.0864
R value (I>2σ(I))	0.0330
Largest diff. peak and hole (e-.Å ⁻³)	1.407 ; -0.593

IV. Catalysis

Catalytic experiments were carried out in a glass vial (3 mL) containing 1 mL of acetonitrile, 1 mM of [FeDPPyCl₂] (1 eq.) and 800 mM of substrate. The reaction was started by adding 20 eq. of PhIO to the solution. After stirring for the desired reaction time at room temperature, 3 μL of internal standard solution (2 mM final) were added to the reaction mixture. The resulting solution was filtered through a short silica gel column. 1.5 mL MeOH were used to collect all remaining organic products. The obtained solution was injected into HPGC to detect and quantify the oxidized products. Conversions were determined by GC against internal standards and calculated relatively to the PhIO as a limiting reagent.

Table S3: Catalytic oxidation activity of [FeDPPyCl₂]. [FeDPPyCl₂]/PhIO/Substrate 1:20:800 eq.

Substrate	Reaction Time	Products	Conversion rel. to PhIO	TON_{max}
PPh ₃	<1min	O=PPh ₃	100 %	20
SPhMe	2h	O=SPhMe	95 %	19
cyclooctene	2/24h	cyclooctene oxide	30 / 46 %	9.2
cyclohexene [‡]	2h	cyclohexene oxide	12 %	3.2
		cyclohexenol	4 %	
toluene	2h/24h	benzyl alcohol	51 % / 93 %	20
		benzaldehyde	1 % / 7 %	
diphenylmethane	24h	diphenylmethanol	15 %	6.2
		benzophenone	8 %	
cyclohexane	24h	cyclohexanol	3 %	1.4
		cyclohexanone	2 %	

[‡] the solvent was degassed prior experiment

V. UV-visible Absorption spectroscopy

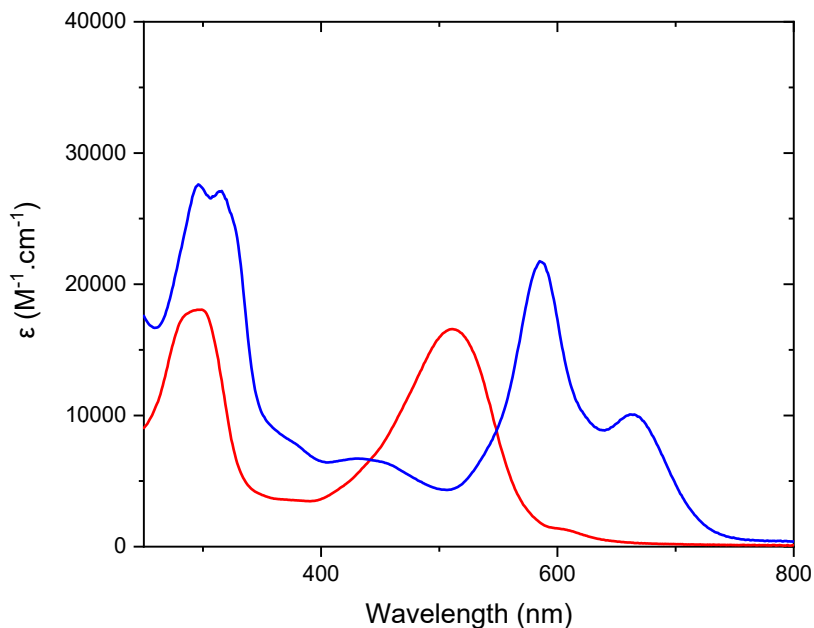


Figure S5: UV-visible spectra of DPPy ligand (red) and $[FeDPPyCl_2]$ (blue) in acetonitrile.

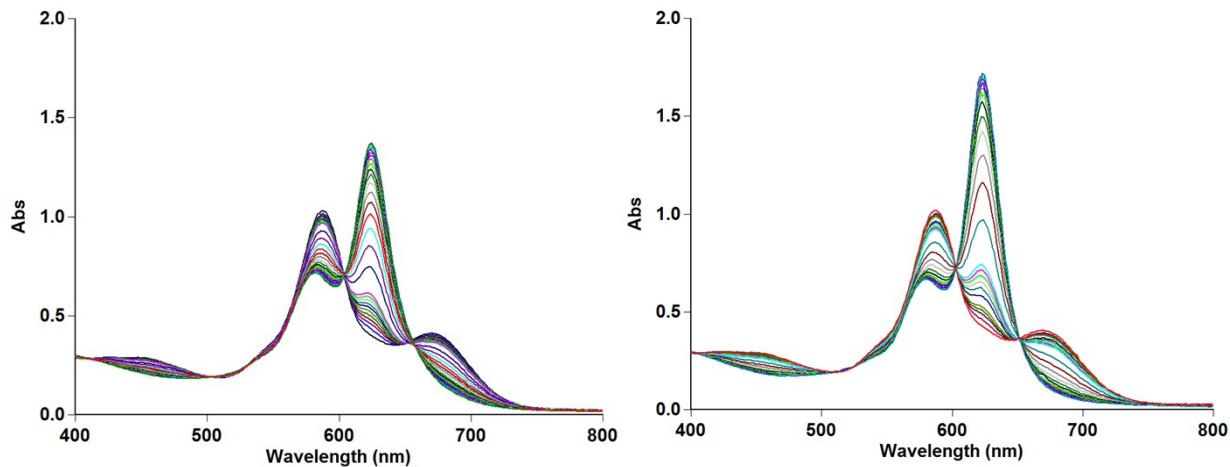


Figure S6: UV-visible spectral changes observed with a $[FeDPPyCl_2]$ solution in ACN upon addition of ca. 1eq (left) or 2 eq (right) of PhIO in MeOH at -40°C. 10 spectra /min between $t=0$ and 1min, then 1 spectrum /min until maximum is reached.

The previous experiments were performed to assess the number of PhIO equivalent needed to generate the detected active species. The small conversion increase observed from addition of 1 to 2eq of PhIO is probably due to an overestimation of the concentration of the prepared PhIO solution, this reagent being known to be very difficult to purify. We can thus assume that one equivalent of PhIO only is needed to generate the active species.

VI. EPR spectroscopy

The experimental spectrum of $[\text{FeDPPyCl}_2]$ could be fitted with a 1:1 mixture of two high spin ($S = 5/2$) iron(III) species probably corresponding to two different geometries. The first set is characterized by three signals at $g = 5.1$, 3.7 and 2.0 ($E/D=0.27$) while the second one is characterized by three signals at $g = 9.1$, 4.2 and 3 ($E/D=0.18$).

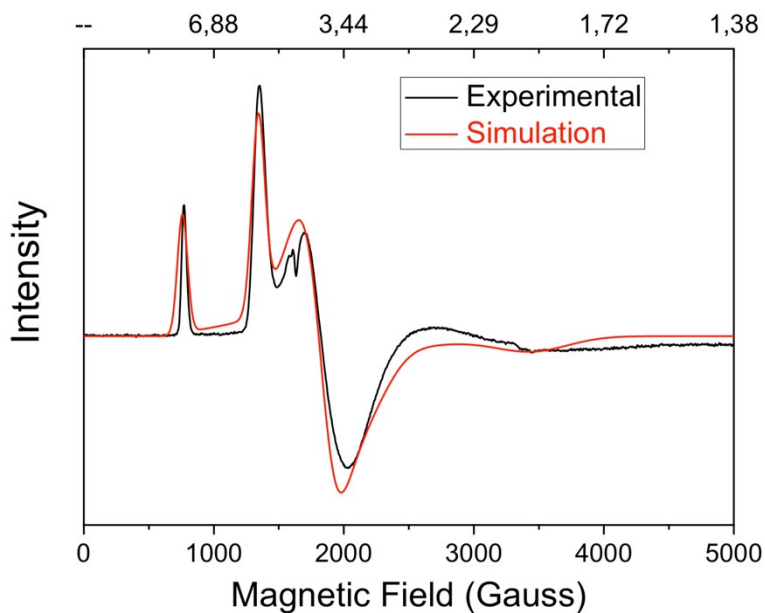


Figure S7: EPR spectrum of $[\text{FeDPPyCl}_2]$ (1 mM) in acetonitrile in presence of TBAPF_6 (0.1 mM) (cavity signal subtracted) and its simulation. Experimental conditions: Microwave power 0.250 mW, microwave freq. 9.63 GHz, modulation amplitude 8 Gauss, gain 44 dB, temperature 10 K.

The experimental spectrum of the oxidized complex could be fitted with a high spin ($S = 5/2$) iron(III) species with $g = 4.28$ ($E/D=0.33$).

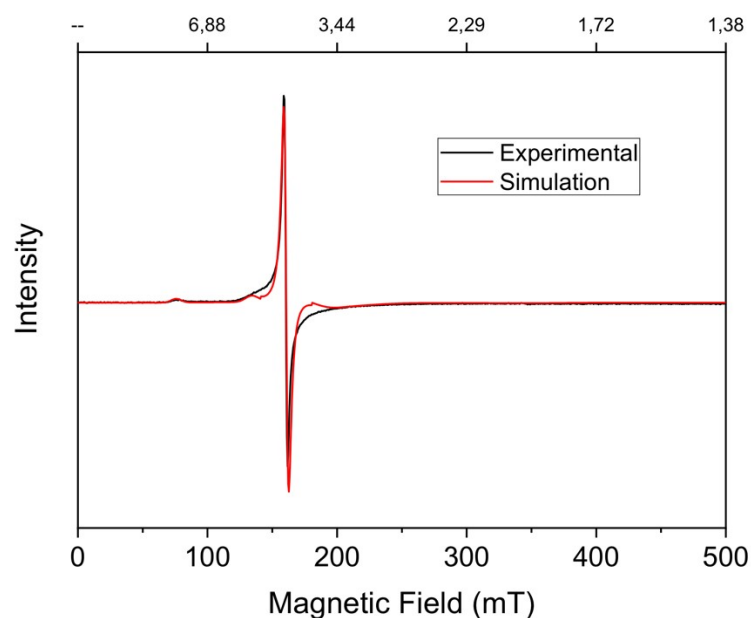


Figure S8: EPR spectrum of $[\text{FeDPPyCl}_2]$ (1 mM) in acetonitrile in presence of TBAPF_6 (0.1 mM) at 10 K after oxidation by PhIO and its simulation (red); Microwave power 0.250 mW, microwave freq. 9.63 GHz, modulation amplitude 8 Gauss, gain 44 dB, temperature 10 K.

VII. Mössbauer spectroscopy

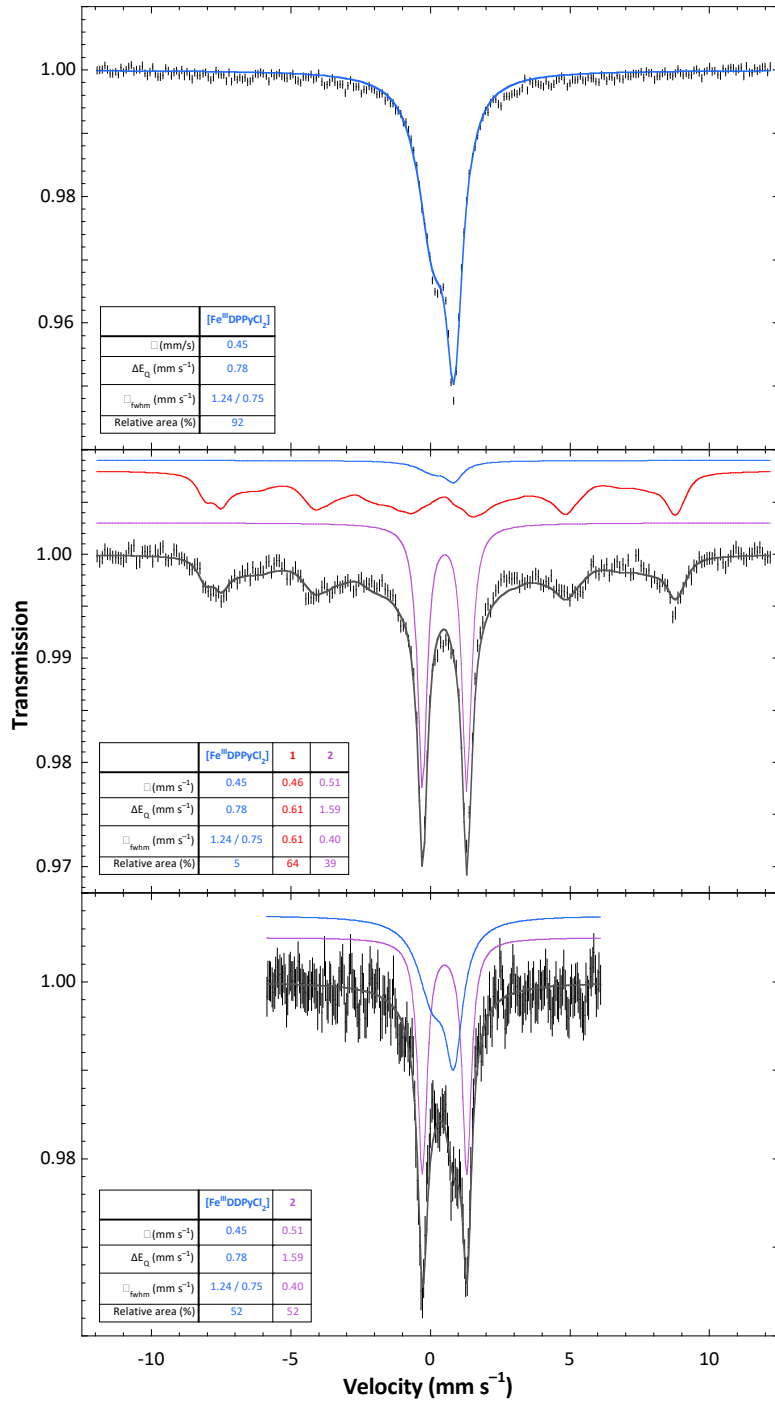


Figure S9: Experimental Mössbauer spectra (hatched bars) recorded at 4.2 (bottom) and 5.8 K (top and middle) using a 0.06 T external magnetic field applied parallel to the γ -beam. Spectra were recorded on frozen solutions of [$^{57}\text{Fe}\text{DPPyCl}_2$] in acetonitrile (2 mM) (top), 10 min after oxidation by PhIO (middle), and after additional 2 h at room temperature (bottom). A simultaneous monitoring of the reaction was performed by UV-visible in order to take samples corresponding to the green and red spectra reproduced on the left part of Figure 2. Simulations are overlaid on experimental spectra as thick solid lines and deconvolutions are displayed above. The starting species (in blue) is well-described by a doublet with two different linewidths.⁷ Species 2 (in mauve) was simulated by a doublet whereas species 1 (in red) was simulated assuming a $S=5/2$ spin state. Species 1 is tentatively assigned to the transient species I.

VIII. Mass spectrometry

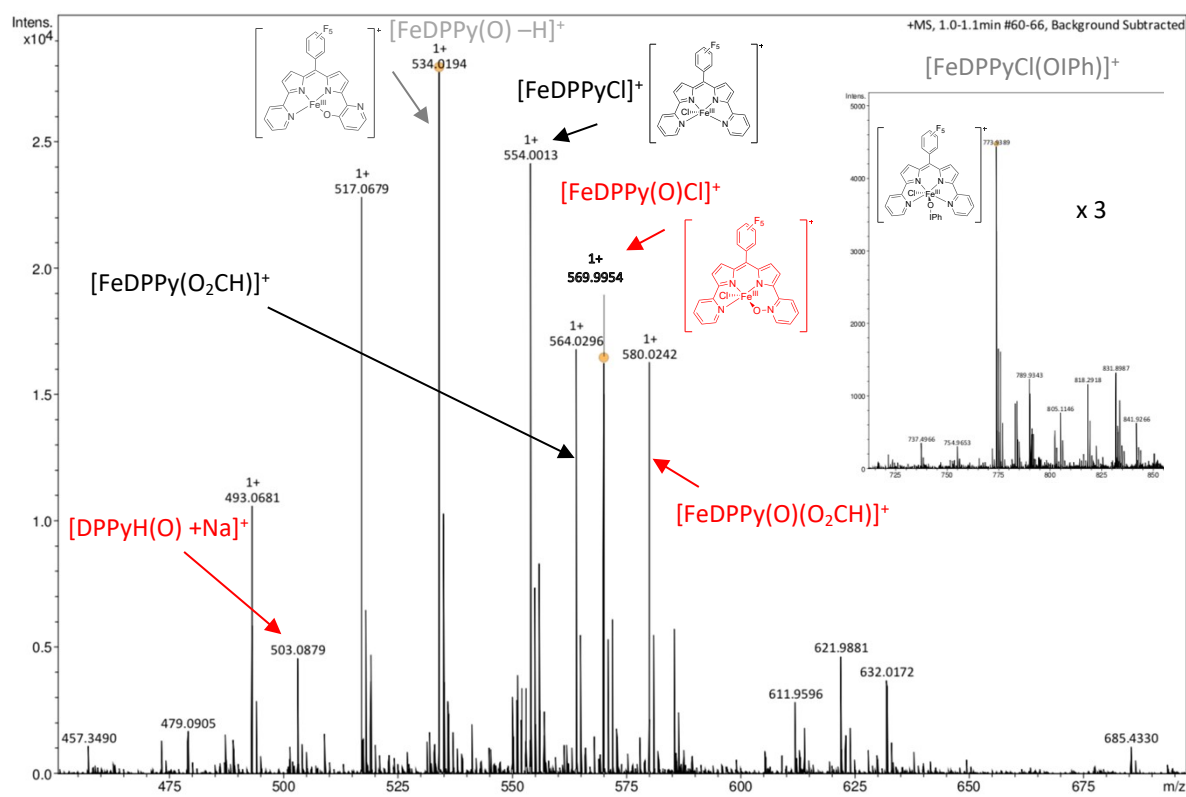


Figure S10: ESI⁺-HRMS analyses and possible assignment of the oxidation products obtained from the reaction of [FeDPPyCl]₂ with PhIO in acetonitrile. Formiate adducts result from anion exchange with the calibrant, sodium formate.

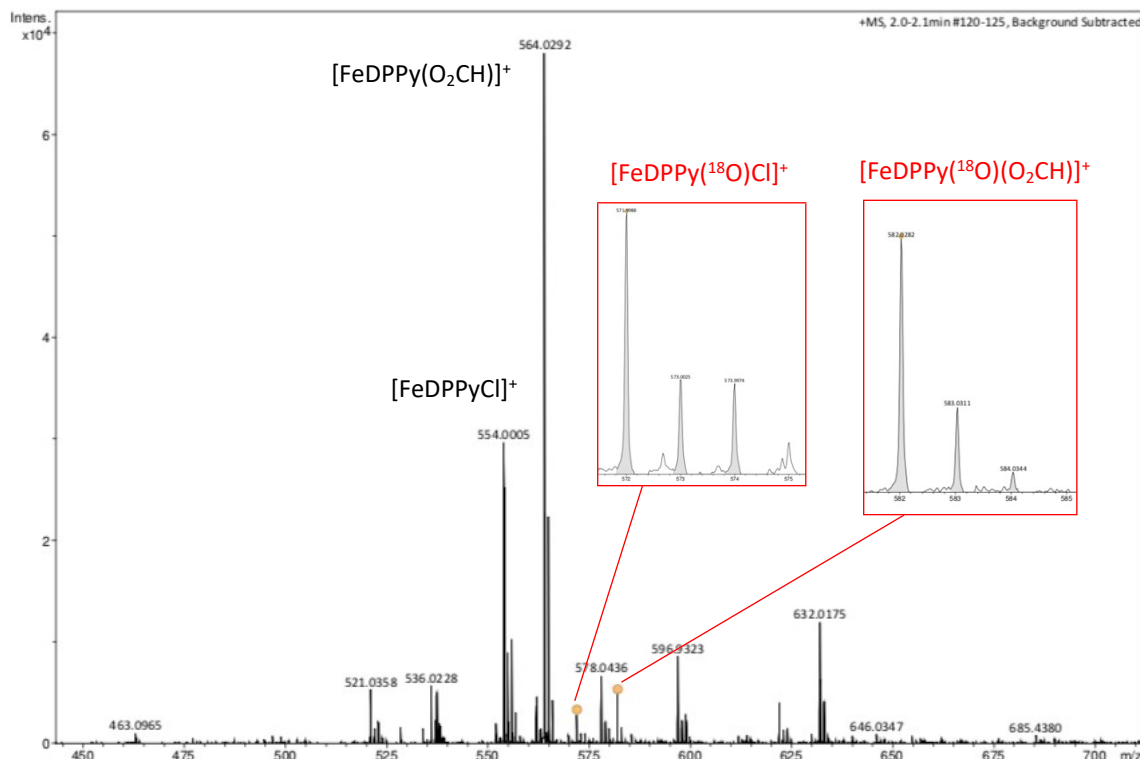


Figure S11: ESI⁺-HRMS analyses showing isotopic shifts upon addition of H₂¹⁸O to the previous sample

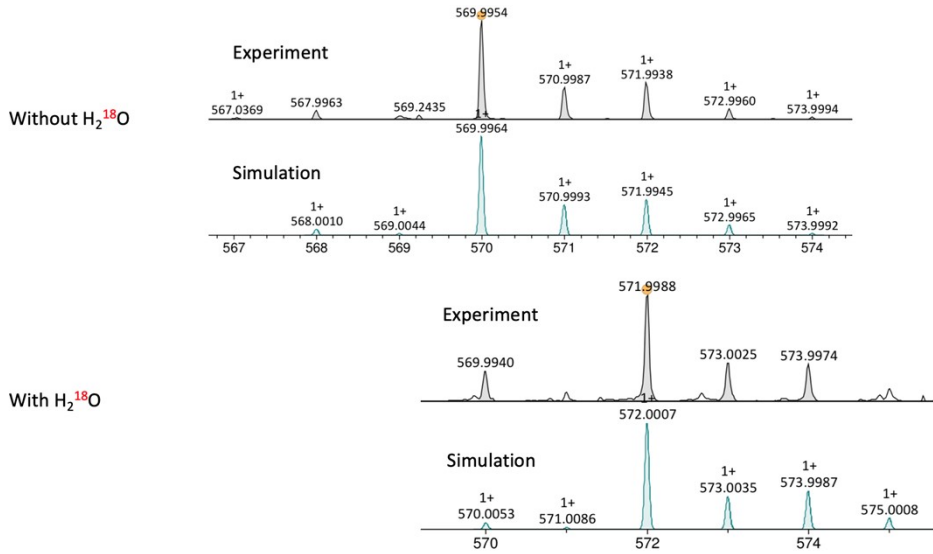


Figure S12: Zoom on the isotopic peak distribution corresponding to $[FeDPPy(O)Cl]^+$ in the absence and presence of $H_2^{18}O$.

IX. Infra-Red spectroscopy

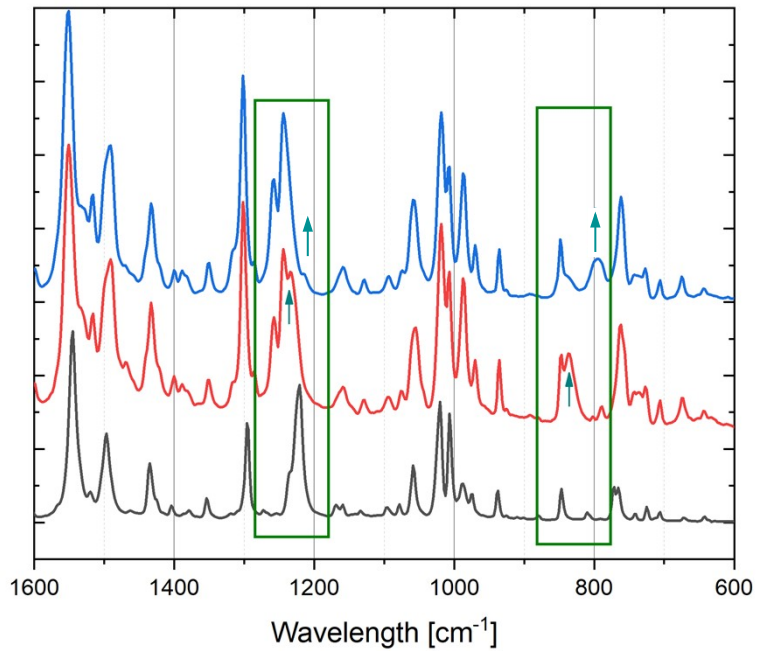


Figure S13: Infrared spectra of a solution of $[FeDPPyCl_2]$ before (black), after addition of PhIO (red), followed by addition of $H_2^{18}O$ (blue).

X. Reactivity with NaClO

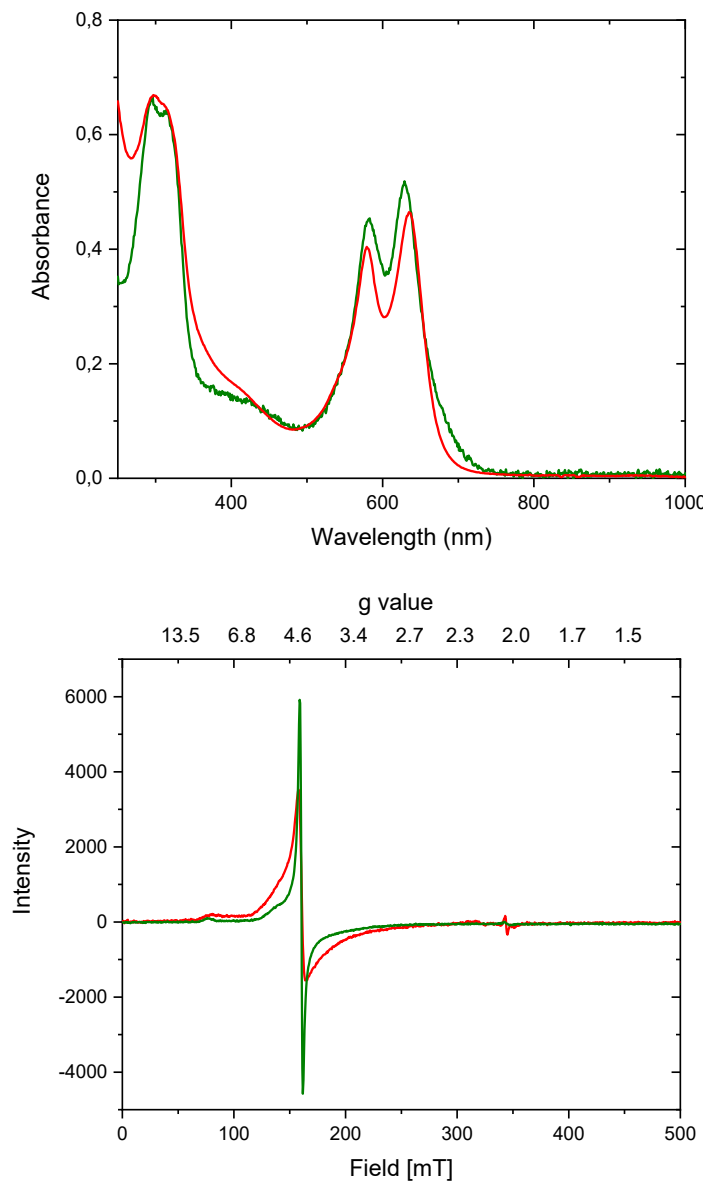


Figure S14: Comparison of the spectroscopic features of the species formed upon oxidation of $[FeDPPyCl_2]$ by PhIO (red) and NaClO (green) monitored by UV-vis (top) and EPR (bottom) spectroscopies.

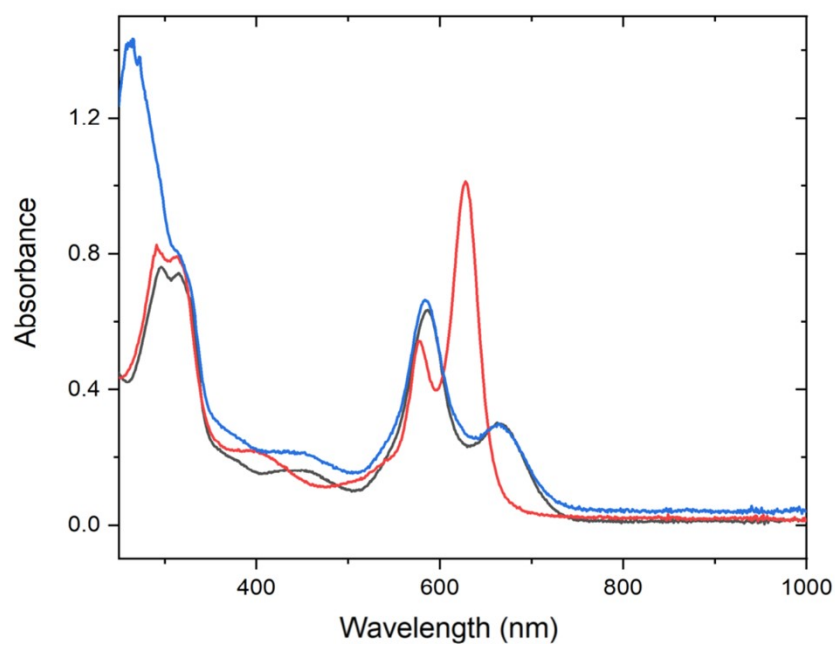


Figure S15: UV-vis spectra of a $[FeDPPyCl_2]$ solution in ACN, before (blue) and after oxidation by $NaClO$ (red) followed by its reaction with PPh_3 (black).

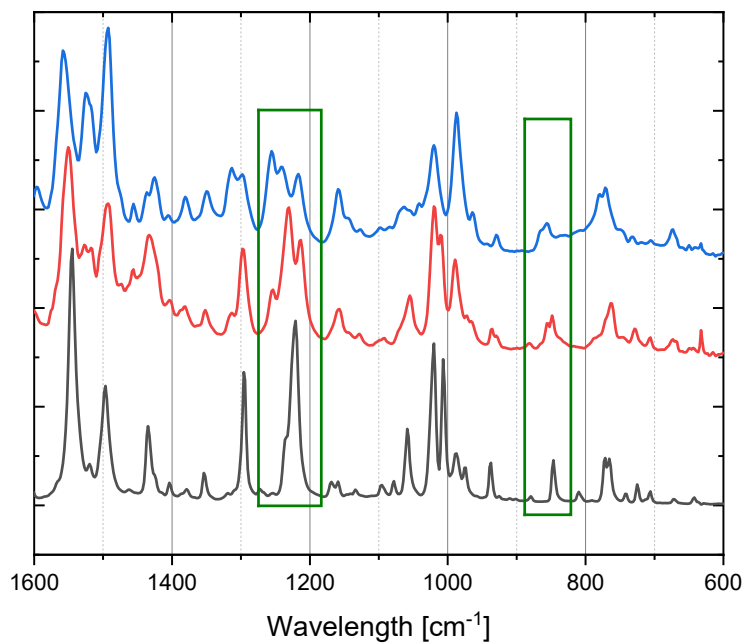


Figure S16: Infrared spectra of $[FeDPPyCl_2]$ precursor (black), after adding $NaClO$ (red) then $H_2^{18}O$ (blue).

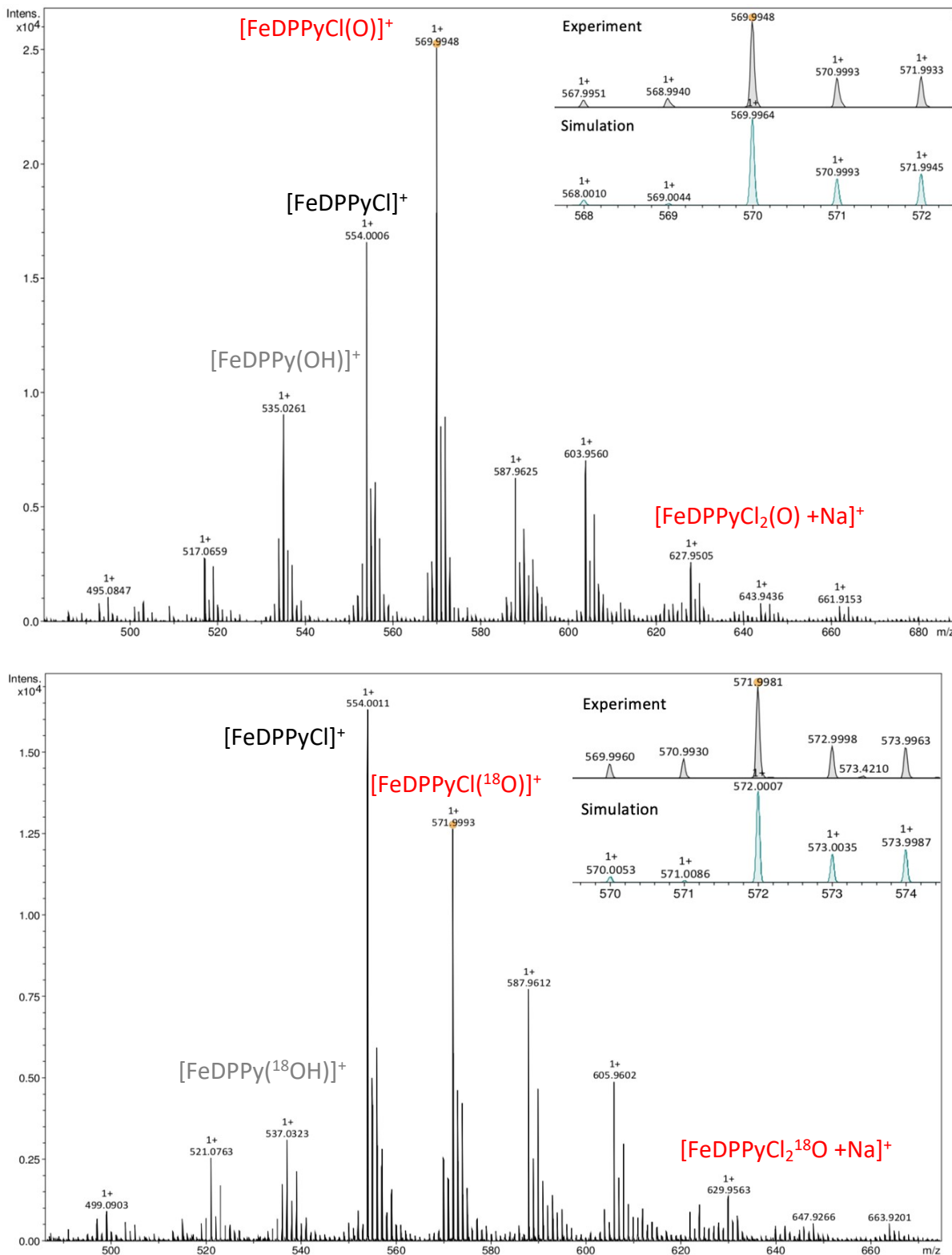


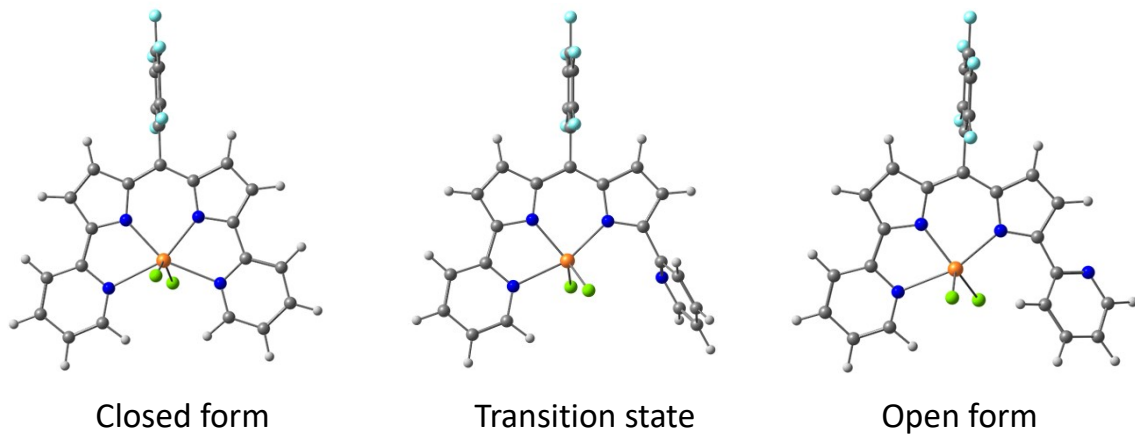
Figure S17: ESI⁺-HRMS analyses of $[\text{FeDPPyCl}_2] + \text{NaClO}$ frozen solution in acetonitrile with H_2^{16}O (Top) with H_2^{16}O H_2^{18}O (Bottom). Inset: Experimental and simulated isotopic distribution of detected species at $m/z = 569.9948$ and 571.9981 .

XI. DFT Calculations

Calculations are based on the density functional theory (DFT) and were performed with Gaussian 09 software package.⁸ Geometries were optimized in the gas phase, using the B3LYP⁹ functional which is known to perform well in IR prediction,¹⁰ in combination with TZVP¹¹ (H,C,N,O,Cl,Fe) and the ECP implemented def2-SVP(l)¹² basis sets. Optimizations were followed by vibrational analysis to confirm the nature of minima or transition states and predict IR spectra. Figures of the structures were performed using ChemCraft or Mercury program. IR spectra were generated by convoluting the theoretical stick spectra with a gaussian fit available in Chemcraft.

Table S4: Comparison of some structural parameters between the geometry optimized ${}^5[FeDPPyCl_2]$ and the X-ray characterized structures, distances in Angstrom, angles in degree.

	B3LYP/TZVP	XRD (form A)	XRD (form B)	XRD (form C)
d(Fe-N3)	2.343	2.235	2.207	2.240
d(Fe-N4)	2.343	2.235	2.238	2.240
d(Fe-N1)	2.113	2.048	2.047	2.076
d(Fe-N2)	2.113	2.048	2.073	2.076
d(Fe-Cl1)	2.299	2.317	2.326	2.302
d(Fe-Cl2)	2.299	2.317	2.308	2.302
A(N1-Fe-N2)	81.9	82.5	81.5	81.2
A(N1-Fe-N3)	72.9	75.2	74.16	75.4
A(N2-Fe-N4)	72.9	75.2	74.16	75.3
A(N3-Fe-N4)	132.2	127.1	127.2	131.4
A(Cl1-Fe-Cl1)	143.8	152	151.1	147.3



	E (H)	ΔE (kcal/mol)	G (H)	ΔG (kcal/mol)
Closed form	-3862.9833	0.0	-3862.7304	0.0
TS	-3862.9686	9.3	-3862.7159	9.1
Open form	-3862.9748	5.4	-3862.7224	5.0

Figure S18: DFT optimized structures and energies of the closed and open forms of $[FeDPPyCl_2]$, as well as the transition state associated with the decoordination of one pyridine arm.

For the decoordination of one pyridine arm, an associated rate constant of 10^7 can be expected, based on the Eyring equation at 298K.

The structure of the computed $[Fe(DPPyO)Cl_2]$ species is given in the article (Fig. 3). Of note, isomers resulting from O insertion in one of the pyrrolic-Fe bond or oxidation of a pendant pyridine arm were calculated respectively 7 and 3 kcal/mol higher in energy.

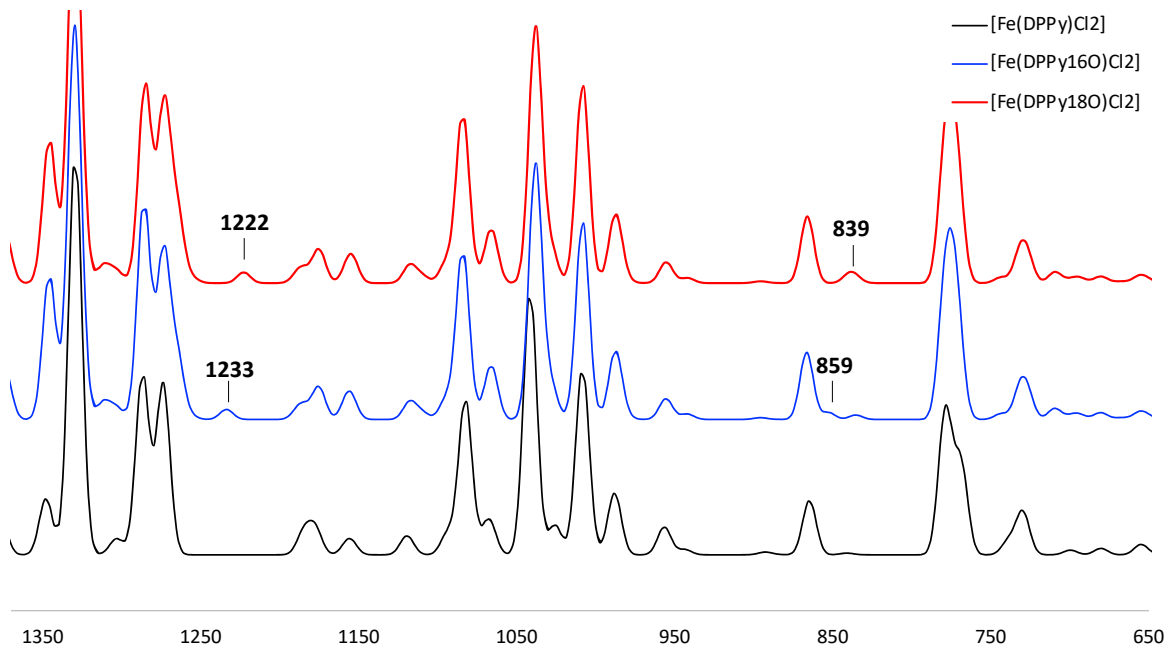


Figure S19: Comparison of the IR spectra calculated for $[FeDPPyCl_2]$ and $[Fe(DPPyO)Cl_2]$. No scaling correction applied, $W_{1/2}=10$ Gaussian broadening.

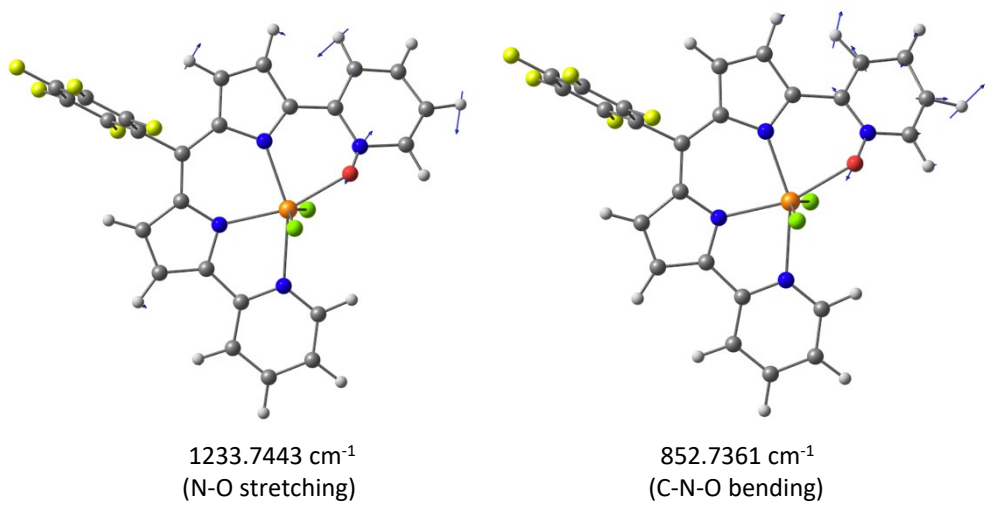


Figure S20: Scaled displacement vectors related to the main vibration modes of the N-O bond calculated for $Fe(DPPy^{16}O)Cl_2$.

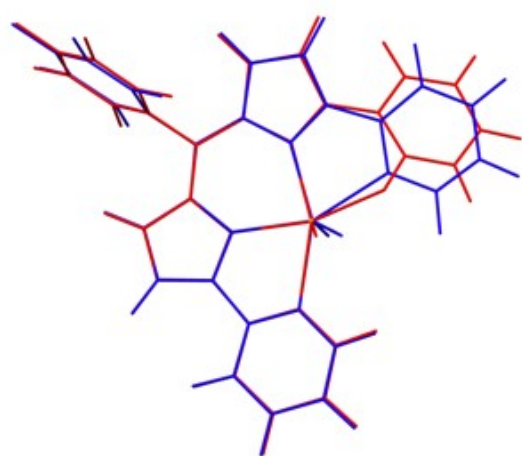


Figure S21: Overlay of the computed structures of $[FeDPPyCl_2]$ (blue) and $[Fe(DPPyO)Cl_2]$ (red).

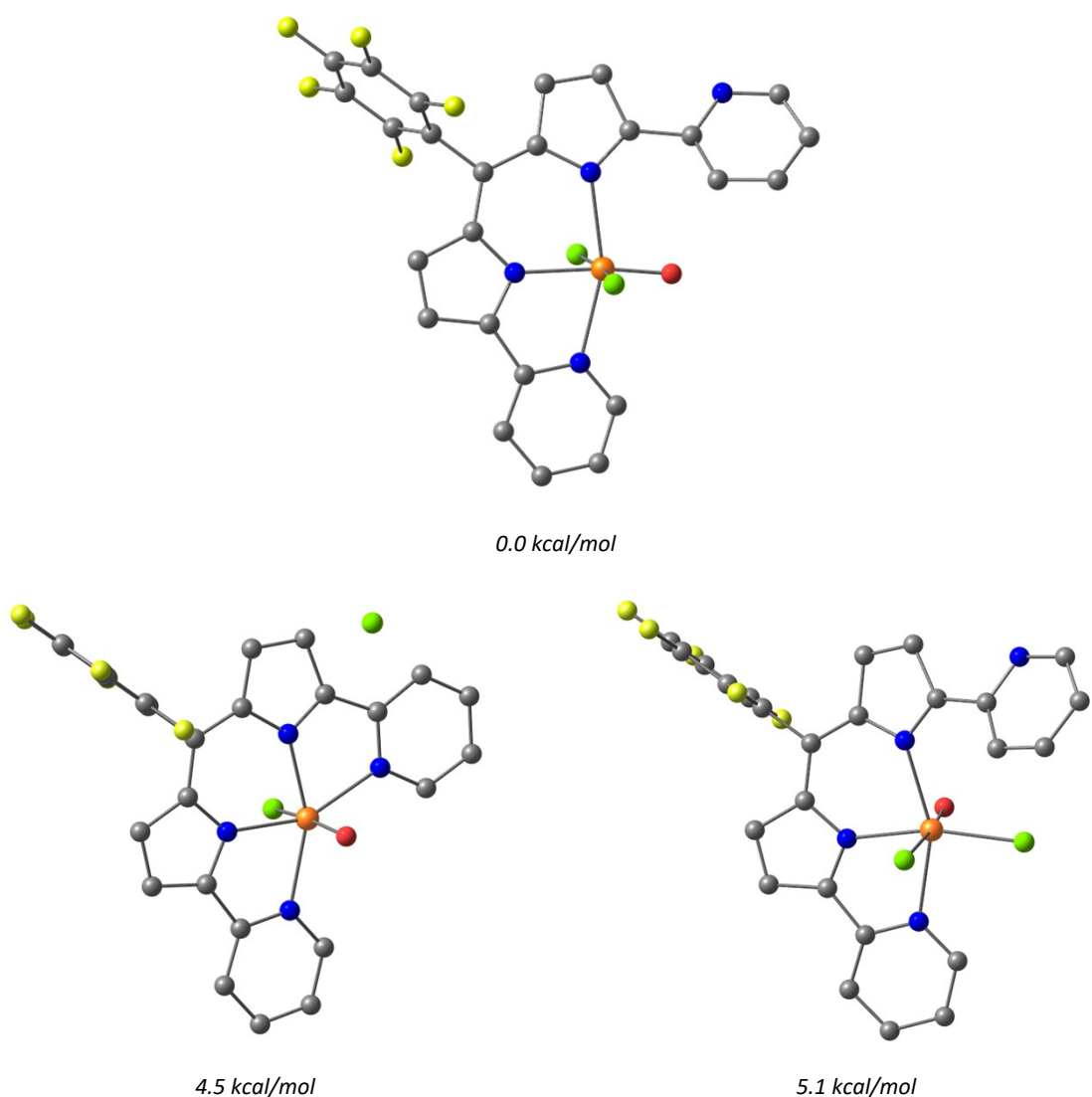


Figure S22 Computed structures for the notional $[Fe^{\nu=O}(DPPy)Cl_2]$, $S=5/2$ structures. H omitted, C grey, O red, N blue, F yellow, Cl green, Fe orange, I purple.

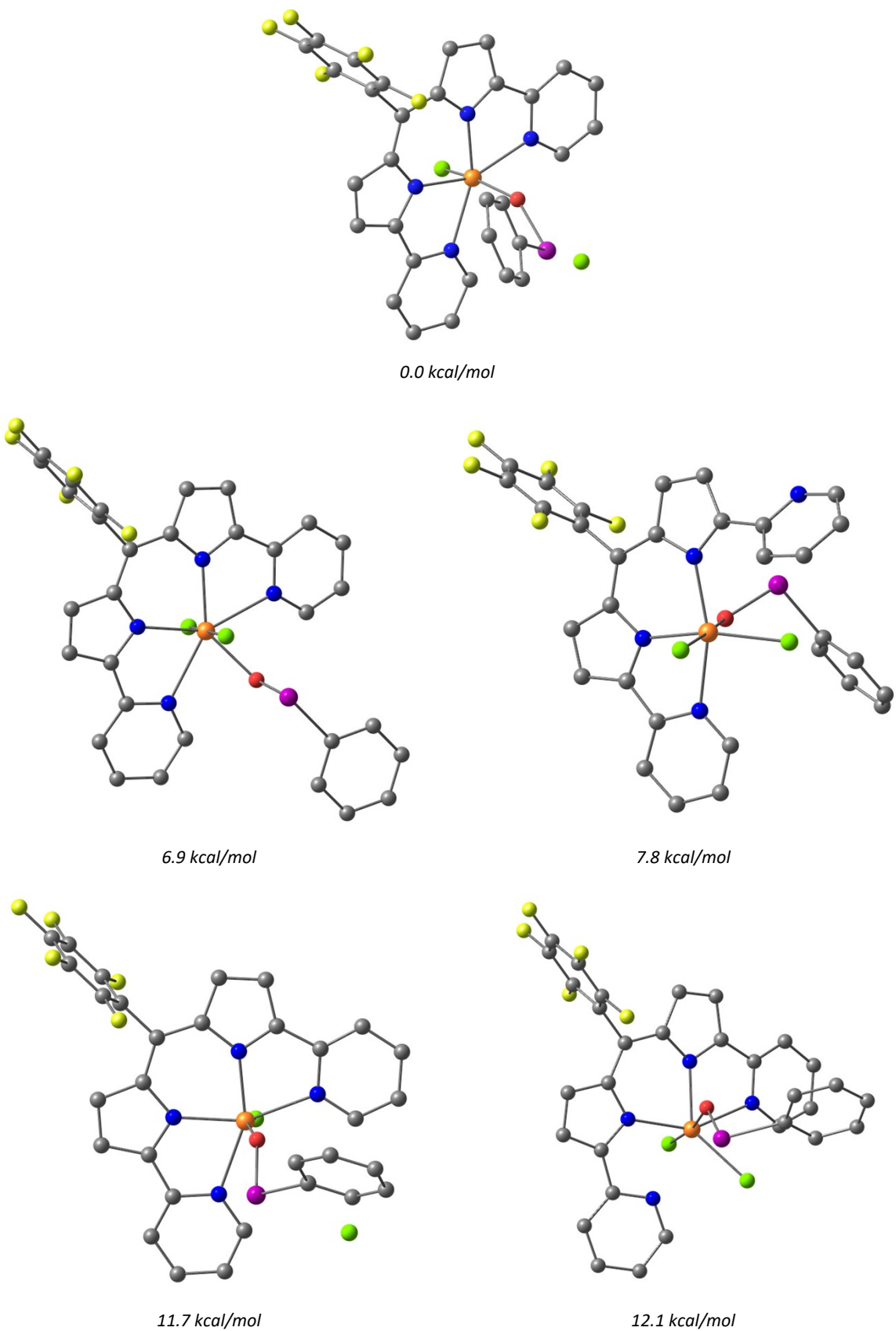


Figure S23 Computed structures for the notional $[FeDPPyCl_2(OIPh)]$, $S=5/2$ structures with their relative free energies. H omitted, C grey, O red, N blue, F yellow, Cl green, Fe orange.

Table S5 Coordinates of the most stable optimized geometries in their lower spin state, UB3LYP energies and thermal free energy at 298K.

[FeDPPyCl₂]

Sextet								
E(UB3LYP) = -3862.98334247 H								
G = -3862.730383 H								
26 -2.020274000 0.000008000 0.000023000	9	3.150886000	-0.140815633	-2.364802000				
6 5.898701000 -0.000001000 -0.000005000	6	3.790294000	-0.139085633	-1.191010000				
17 -2.733317000 0.000899000 2.185805000	7	-0.327111000	1.572251000	0.008326367				
9 7.231582000 -0.000001000 -0.000006000	6	1.025104000	1.326787000	-0.014585266				
9 5.872946000 0.000733000 -2.357362000	6	1.571707000	0.029230000	-0.006696633				
6 5.203605000 0.000368000 -1.201874000	6	3.066662000	-0.063293000	-0.004174000				
9 3.173539000 0.000728000 -2.362350000	7	-2.792313000	2.454852000	0.066022266				
6 3.814999000 0.000352000 -1.189501000	6	1.713875000	2.568441000	-0.024910899				
7 -0.423879000 1.384597000 0.000376000	1	2.783632000	2.699749000	-0.041817532				
6 0.948617000 1.238040000 0.000514000	6	-0.492664000	2.912404000	0.013627367				
6 1.595158000 0.000002000 -0.000004000	6	0.755951000	3.566793000	-0.005731899				
6 3.091138000 0.000001000 -0.000005000	1	0.927747000	4.631013000	-0.006544899				
7 -2.968858000 2.142132000 -0.000708000	6	-1.851076000	3.418208000	0.048377000				
6 1.548744000 2.535699000 0.000875000	6	-2.200329000	4.770619000	0.065317000				
1 2.606873000 2.742055000 0.001048000	1	-1.430964000	5.530202000	0.049252367				
6 -0.679855000 2.699293000 0.000623000	6	-4.081722000	2.785071000	0.102749899				
6 0.525853000 3.452997000 0.001038000	1	-4.784268000	1.961934000	0.116523165				
1 0.614849000 4.527207000 0.001289000	9	5.841394000	-0.138740367	2.359913000				
6 -2.064321000 3.137416000 0.000158000	6	5.174599000	-0.137710000	1.203068000				
6 -2.458857000 4.478075000 0.000420000	9	3.146015000	0.012191633	2.357083000				
1 -1.715231000 5.262984000 0.001161000	6	3.788366000	-0.060452000	1.186320000				
6 -3.811402000 4.778581000 -0.000282000	7	-0.541056000	-1.273058633	-0.009091633				
1 -4.141315000 5.809898000 -0.000084000	6	0.858791000	-1.158244000	0.007779633				
6 -4.737162000 3.740453000 -0.001271000	7	-2.736932330	-3.345209074	-1.181520303				
1 -5.801384000 3.932533000 -0.001891000	6	1.427223000	-2.471066000	0.062955330				
6 -4.265584000 2.434102000 -0.001448000	1	2.480700000	-2.699627367	0.083768596				
1 -4.947749000 1.593435000 -0.002293000	6	-0.809935000	-2.582605000	0.033594431				
9 5.872947000 -0.000734000 2.357351000	6	0.387508000	-3.355790000	0.089610862				
6 5.203606000 -0.000370000 1.201863000	1	0.426399633	-4.434227367	0.122587293				
9 3.173541000 -0.000726000 2.362340000	6	-2.170704367	-3.186378633	0.018078798				
6 3.815000000 -0.000352000 1.189491000	6	-2.756388037	-3.635012558	1.204721633				
7 -0.423882000 -1.384591000 -0.000365000	1	-2.262306340	-3.477052952	2.153507367				
6 0.948615000 -1.238035000 -0.000518000	6	-3.994656670	-4.257537293	1.134650633				
7 -2.968864000 -2.142155000 0.000678000	1	-4.482946606	-4.608444420	2.037010734				
6 1.548743000 -2.535693000 -0.000875000	6	-4.597547633	-4.412720734	-0.106947468				
1 2.606872000 -2.742048000 -0.001048000	1	-5.566791633	-4.888905468	-0.207895468				
6 -0.679855000 -2.699289000 -0.000628000	6	-3.929986330	-3.940220442	-1.231379936				
6 0.525854000 -3.452991000 -0.001053000	1	-4.364493027	-4.042573048	-2.221270037				
1 0.614852000 -4.527201000 -0.001317000	17	-2.961371835	0.037502697	-1.997061431				
6 -2.064316000 -3.137428000 -0.000172000								
6 -2.458835000 -4.478091000 -0.000435000								
1 -1.715200000 -5.262991000 -0.001167000								
6 -3.811377000 -4.778614000 0.000255000								
1 -4.141277000 -5.809935000 0.000058000								
6 -4.737149000 -3.740498000 0.001233000								
1 -5.801369000 -3.932589000 0.001843000								
6 -4.265586000 -2.434140000 0.001407000								
1 -4.947760000 -1.593481000 0.002241000								
17 -2.733369000 -0.000854000 -2.185740000								

{[FeDPPyCl₂]}* pyridine decoordination

Sextet								
E(UB3LYP) = -3862.96855747 H								
G = -3862.715939 H								
One imaginary frequency : -40.7654 cm ⁻¹								
26 -1.957715000 0.335111367 -0.039375532	6	1.957438000	0.366005000	-0.096090000				
6 5.869862000 -0.216284000 0.003704000	6	-5.839614000	-0.185619000	-0.000549000				
17 -3.120514165 -0.197770798 1.798793936	17	2.723403000	0.284047000	-2.205161000				
9 7.200426000 -0.289729000 0.007628000	9	-7.170254000	-0.256015000	0.002335000				
9 5.846079000 -0.290118633 -2.352218000	9	-5.830385000	0.232186000	2.319730000				
6 5.176939000 -0.218140000 -1.199476000	6	-5.154095000	0.065209000	1.180704000				
	9	-3.136157000	0.375187000	2.319677000				
	6	-3.767741000	0.138598000	1.164905000				
	7	0.351327000	1.598832000	0.043015000				
	6	-0.997706000	1.353882000	-0.023097000				
	6	-1.540363000	0.052284000	-0.012490000				
	6	-3.034834000	-0.038883000	-0.006050000				
	7	2.817392000	2.474295000	0.112397000				
	6	-1.683605000	2.593827000	-0.068112000				
	1	-2.751860000	2.726013000	-0.124034000				
	6	0.520766000	2.941614000	0.040317000				
	6	-0.724541000	3.593589000	-0.027117000				
	1	-0.896521000	4.657670000	-0.043760000				

6	1.879050000	3.441728000	0.098734000		1	-2.589636282	2.705556228	0.087089685
6	2.233484000	4.792294000	0.145785000		6	0.780273826	2.607055000	0.070685772
1	1.466755000	5.554708000	0.136660000		6	-0.468837685	3.335433946	0.054671000
6	3.576118000	5.128655000	0.204231000		1	-0.564782826	4.406129718	0.052802228
1	3.874967000	6.168859000	0.239963000		6	2.156556108	3.137410174	-0.026075631
6	4.534881000	4.119279000	0.220600000		6	2.379427021	4.347763120	-0.607901946
1	5.591259000	4.344539000	0.268669000		1	1.421896228	4.774425099	-0.889221925
6	4.107416000	2.799683000	0.173937000		6	3.552394456	5.030886424	-0.815289598
1	4.806827000	1.973887000	0.191146000		1	3.700323141	5.986275967	-1.290634826
9	-5.795904000	-0.599500000	-2.320797000		6	4.505225153	4.175883033	-0.299030631
6	-5.136404000	-0.362134000	-1.184565000		1	5.565654663	4.402155729	-0.390170402
9	-3.102148000	-0.457434000	-2.332307000		6	4.370390033	2.971745174	0.272032913
6	-3.749664000	-0.288117000	-1.174970000		1	5.173066402	2.338197631	0.607815402
7	0.569659000	-1.279413000	-0.039034000		8	3.090541141	1.484569619	0.976686033
6	-0.829346000	-1.135403000	0.020151000		17	2.917583000	0.174871000	-1.792316000
7	2.199388000	-4.332453000	0.914411000					
6	-1.418658000	-2.431220000	0.202992000					
1	-2.474748000	-2.631371000	0.279683000					
6	0.813442000	-2.592633000	0.112300000					
6	-0.400484000	-3.328889000	0.285897000					
1	-0.447750000	-4.392942000	0.441242000					
6	2.118869000	-3.275894000	0.086218000					
6	3.156354000	-2.926797000	-0.779726000					
1	3.046633000	-2.103080000	-1.468513000					
6	4.327672000	-3.670663000	-0.750768000					
1	5.146006000	-3.418783000	-1.413821000					
6	4.429141000	-4.736093000	0.132358000					
1	5.325987000	-5.339343000	0.190802000					
6	3.331525000	-5.027119000	0.939051000					
1	3.362277000	-5.862692000	1.631029000					
17	3.294013000	-0.295771000	1.568198000					
Fe(DPPy¹⁶O)Cl₂								
Sextet								
E(UB3LYP) = -3938.17018177 H								
G = -3937.912925 H								
26	1.943173000	-0.243611000	0.302443000					
6	-5.909878000	0.157789000	-0.026818772					
17	1.895763000	-0.863121000	2.527138000					
9	-7.241506000	0.217247000	-0.031358000					
9	-5.886743000	0.096251000	-2.392647228					
6	-5.221377228	0.094187000	-1.228128772					
9	-3.191560000	-0.023255000	-2.394116000					
6	-3.829874000	0.035085228	-1.220116000					
7	0.312373087	-1.500901228	-0.196459000					
6	-1.040591456	-1.281819315	-0.189877228					
6	-1.605234772	-0.008549402	-0.014957315					
6	-3.099918772	0.013463087	-0.035875228					
7	2.833722000	-2.335238772	-0.027070000					
6	-1.672375544	-2.564347000	-0.351336000					
1	-2.732436315	-2.749110913	-0.385455000					
6	0.538567772	-2.812546456	-0.343570000					
6	-0.684308544	-3.522502685	-0.457619000					
1	-0.824364228	-4.585262685	-0.590829228					
6	1.914395000	-3.284744000	-0.303961000					
6	2.283641000	-4.617980228	-0.521401000					
1	1.530371000	-5.360026228	-0.747689000					
6	3.624223000	-4.958105000	-0.444853000					
1	3.938879228	-5.982537000	-0.608378000					
6	4.562928000	-3.973133000	-0.158719000					
1	5.613344772	-4.201417000	-0.091194000					
6	4.123334228	-2.667133772	0.039404000					
1	4.819871456	-1.867737000	0.256473000					
9	-5.881121000	0.217776000	2.324784000					
6	-5.209243772	0.159280000	1.174340228					
9	-3.185760000	0.098227000	2.330005000					
6	-3.817323544	0.103019228	1.153520772					
7	0.478190685	1.313575141	0.126577228					
6	-0.923244685	1.196485141	0.084987544					
7	3.188623456	2.499392000	0.393615772					
6	-1.535551282	2.468405544	0.080515000					

[FeDPPy(O)Cl₂]

Quartet

E(UB3LYP) = -3938.11094925 H

G = -3937.857327 H

26	2.088669000	-0.307154000	-0.172854000
17	2.364505000	-0.234102000	2.179385000
7	0.454913000	-1.522529000	0.203292000
7	2.917914000	-2.392655000	-0.066100000
7	0.560217000	1.380926000	-0.040051000
8	3.480751000	0.485228000	-0.484979000
17	1.551785000	-0.585889000	-2.420002000
6	-0.890313000	-1.288094000	0.290350000
6	0.653819000	-2.820036000	0.381628000
6	-1.482382000	-0.042814000	0.063475000
6	-1.564251000	-2.547790000	0.579990000
6	-2.978524000	0.001019000	0.058916000
6	-3.719292000	-0.497762000	-1.011300000
6	-5.107590000	-0.462484000	-1.020084000
6	-5.786092000	0.077211000	0.064815000
9	-7.116853000	0.112852000	0.067665000
6	-5.075219000	0.578226000	1.147698000
9	-5.791757000	-0.941512000	-2.060172000
9	-3.095050000	-1.020054000	-2.069907000
6	-0.804014000	1.163603000	-0.171348000
6	-3.687726000	0.536703000	1.132666000
6	2.003441000	-3.332551000	0.252033000
6	4.185835000	-2.736029000	-0.232716000
1	-2.624642000	-2.675916000	0.720819000
6	-0.603741000	-3.501963000	0.635372000
1	-0.733850000	-4.554787000	0.826237000
6	2.357731000	-4.671751000	0.412983000
1	1.610238000	-5.410366000	0.668316000
6	3.688254000	-5.032173000	0.239571000
1	3.993571000	-6.063848000	0.359223000
6	4.617738000	-4.054943000	-0.089668000
1	5.661606000	-4.298743000	-0.233515000
1	4.863794000	-1.930192000	-0.485418000
9	-5.727853000	1.091730000	2.191647000
9	-3.030606000	1.021628000	2.190639000
6	0.751336000	2.675464000	-0.279106000
6	-1.465153000	2.404503000	-0.554991000
7	2.035856000	4.580349000	-0.806655000
6	1.991424000	3.418288000	-0.118303000
6	3.128133000	5.320407000	-0.706304000
1	-2.520477000	2.522763000	-0.735480000
6	-0.501552000	3.339300000	-0.651758000
1	-0.579159000	4.379364000	-0.917772000
6	3.019470000	3.005225000	0.739664000
1	2.927775000	2.093794000	1.312168000
6	4.147472000	3.808049000	0.845408000
1	4.958923000	3.515400000	1.499320000
6	4.215885000	4.976691000	0.102878000
1	5.080601000	5.626243000	0.152521000
1	3.141914000	6.238081000	-1.285355000

[FeDPPyCl(OlPh)]Cl							
Sextet				6	4.402179000	0.611506000	0.848118000
E(UB3LYP) = -4467.66812150 H				7	0.516732000	-1.790054000	0.498532000
G = -4467.336103 H				6	1.858473000	-1.466169000	0.520694000
26	-1.132646000	-1.096511000	-0.628789000	7	-1.945609000	-2.735879000	0.768687000
6	6.652109000	0.241294000	0.105099000	6	2.519452000	-2.324742000	1.454119000
17	-5.174804000	-0.317469000	0.395991000	1	3.571894000	-2.312669000	1.687910000
9	7.961026000	0.461443000	0.222824000	6	0.336276000	-2.797037000	1.361250000
9	7.029529000	-1.183080000	-1.734172000	6	1.564099000	-3.160375000	1.980946000
6	6.174455000	-0.596688000	-0.893599000	1	1.711255000	-3.937374000	2.713344000
9	4.380307000	-1.632661000	-1.976121000	6	-1.002935000	-3.336170000	1.522230000
6	4.808073000	-0.817948000	-1.007488000	6	-1.319949000	-4.387094000	2.382765000
7	0.362327000	0.171492000	-1.428050000	1	-0.546471000	-4.855603000	2.975555000
6	1.715293000	0.309534000	-1.196297000	6	-2.637714000	-4.814274000	2.461379000
6	2.423297000	-0.467857000	-0.275610000	1	-2.908350000	-5.627939000	3.122744000
6	3.892509000	-0.221906000	-0.143439000	6	-3.601267000	-4.181429000	1.687706000
7	-2.188913000	0.261164000	-2.188369000	1	-4.641832000	-4.472420000	1.727438000
6	2.223390000	1.335867000	-2.052314000	6	-3.210188000	-3.142369000	0.849191000
1	3.246520000	1.672975000	-2.096145000	1	-3.934831000	-2.599648000	0.256542000
6	0.031533000	1.048807000	-2.383215000	17	-1.285009000	-2.683101000	-2.267583000
6	1.166882000	1.797977000	-2.799599000	6	-1.899878000	4.209717000	1.594944000
1	1.189492000	2.571987000	-3.549441000	6	-0.939771000	5.147038000	1.968190000
6	-1.345609000	1.087022000	-2.842770000	6	-1.562128000	2.860929000	1.570511000
6	-1.785308000	1.888058000	-3.897647000	1	-1.195794000	6.199525000	1.987606000
1	-1.090434000	2.540594000	-4.407868000	6	0.344954000	4.731419000	2.305317000
6	-3.116377000	1.822917000	-4.281513000	6	-0.286087000	2.432503000	1.908241000
1	-3.478484000	2.433632000	-5.099228000	1	1.092235000	5.461422000	2.590964000
6	-3.973324000	0.962161000	-3.608039000	1	-0.041171000	1.379332000	1.878204000
1	-5.019053000	0.881456000	-3.870684000	6	0.670402000	3.378519000	2.271299000
6	-3.466314000	0.195507000	-2.564776000	1	1.670570000	3.052416000	2.528817000
1	-4.107318000	-0.461882000	-1.992195000	1	-2.895911000	4.542760000	1.320797000
9	6.221094000	1.657864000	1.940778000	53	-3.139486000	1.457335000	1.065573000
6	5.763165000	0.849888000	0.980941000	8	-1.879663000	0.076339000	0.744151000
9	3.570648000	1.215799000	1.707496000				

Table S6 Calculated frequencies (cm^{-1}) with their IR intensities at 298K.

[FeDPPyCl ₂] closed form		297.9634	0	739.1427	15.49
10.5208	0	302.7783	0.0038	766.4145	0.0002
24.998	0.0709	313.6707	1.2666	769.015	100.0657
30.88	0	343.783	0.5647	772.9742	0.0005
34.334	0.0975	352.414	122.7091	776.804	29.6756
41.9139	3.1387	382.2636	0.7568	779.4587	137.7033
53.3409	3.507	383.9931	0	841.3345	1.939
60.7047	0	404.7876	10.3705	865.0581	61.7417
65.1986	0.1785	422.2005	7.38	881.1302	0
81.5071	0.8487	429.2602	0	884.5133	0.2029
86.5492	0.5098	432.0852	6.0876	890.5744	0
111.3106	0.2257	442.0094	0.6509	893.0336	3.1166
112.017	0	448.8335	0.1807	944.0226	6.0784
123.5303	0.5468	484.2863	2.7777	954.0501	0
128.5594	4.9692	485.084	0.0005	956.8788	31.3877
131.1056	1.472	486.6201	0.4107	960.6608	0.1794
131.6355	0	527.6344	0.0227	988.3647	69.5065
144.307	1.7417	534.8475	1.6506	991.106	0
172.3002	0.0014	561.6856	0.4491	991.2131	0.632
185.1391	0	586.6799	0.582	1008.6787	212.9742
197.9609	0.5276	648.7162	0.2639	1026.0365	33.5929
201.127	1.6161	651.2475	0	1027.9791	0.2873
210.3295	0.0252	652.2897	1.1712	1041.7669	299.6442
213.4923	0	655.4785	10.8131	1067.6802	38.8122
229.6654	0.0007	664.7501	0	1070.0207	0.1088
239.562	5.8269	678.3515	0	1073.2559	4.2272
255.2482	5.2817	680.5614	7.2926	1082.8322	176.4822
281.1087	0.0522	699.9319	5.316	1094.0341	24.5004
283.7431	0.0339	723.896	0.174	1116.9585	0.4998
289.4331	14.3709	729.5397	28.2453	1119.8006	21.1685
289.8872	24.9264	730.82	21.2683	1155.3563	5.8165
		733.9762	0	1155.9491	9.4379

179.3591	0.501	699.0001	3.1991	1264.9248	71.9119
197.276	0.2527	709.1719	11.4775	1273.3094	181.9731
199.8393	1.4834	726.65	23.083	1285.2761	205.0748
217.0419	1.2083	731.283	29.0819	1298.5201	0.8631
220.9042	9.6199	743.3784	5.9259	1303.7087	12.289
228.8516	0.3226	769.9873	35.0298	1311.626	18.1794
238.6734	7.1943	772.3356	94.0739	1327.307	72.8735
246.0968	1.2532	776.5672	34.8513	1330.2654	346.6245
260.1805	6.2826	777.6106	27.7294	1345.8207	149.1953
281.3571	0.1397	779.4523	83.3535	1374.113	52.1809
283.8151	0.1988	835.3145	5.0187	1405.8785	100.9168
289.3957	15.1164	839.612	8.2109	1434.2596	0.4756
297.8494	10.3279	865.9626	68.7655	1453.1052	89.8643
304.2777	0.3311	869.1672	0.125	1454.7953	19.3702
312.8824	1.2928	888.0652	0.1026	1464.7837	11.9646
327.5958	25.5703	894.2537	0.1335	1474.5641	49.4043
336.2581	107.8077	895.8107	1.7097	1490.431	22.6369
343.2555	8.307	941.774	5.1796	1512.1444	335.0233
370.2241	6.7481	948.9387	0.5353	1518.2497	122.7871
384.239	0.0277	955.4443	21.4838	1524.7186	66.3704
395.3538	1.1968	967.6453	0.0454	1527.2326	213.9701
418.4127	6.5994	980.8969	3.0022	1533.6003	180.5715
422.8778	5.774	987.4252	70.8277	1556.7035	45.5064
432.2469	3.2428	993.0338	0.4615	1587.1313	564.265
448.8747	0.1437	1008.2848	205.7364	1596.0231	94.6947
454.4391	1.3386	1028.3265	35.6048	1612.1395	16.2492
486.2547	0.8765	1038.0982	264.2649	1639.7523	21.7382
490.3672	0.5019	1066.0304	54.5059	1645.9087	5.2789
505.6997	2.237	1071.0297	2.6299	1652.8117	5.1948
518.6859	2.0204	1074.4825	0.9812	1667.8554	29.5529
529.865	0.8547	1084.1379	176.4037	3186.6571	8.9121
563.8062	8.0663	1094.6154	21.2587	3193.3796	1.2776
565.704	4.3227	1109.8466	7.2532	3202.0055	3.4581
586.1053	0.6413	1117.6565	18.539	3208.1206	5.2899
593.5837	7.0812	1153.7848	8.6755	3213.8367	8.1347
650.6118	2.9664	1155.0464	18.7455	3218.1179	1.0691
655.2439	5.678	1158.0343	4.2267	3228.9435	0.1531
657.943	1.5306	1175.2259	34.6598	3240.6488	2.5339
667.6256	1.6839	1184.7761	10.716	3243.5644	2.8692
678.7326	3.6861	1188.6174	7.6751	3254.9728	1.6784
681.7433	3.6362	1222.8435	11.0955	3257.1105	5.0388
693.588	4.9211	1255.6808	5.3597	3260.2012	4.2946

References

- ¹ G. M. Sheldrick, *SHELXS-97*, Program for Crystal Structure Solution, University of Göttingen, Göttingen, Germany, 1997
- ² G. M. Sheldrick, *Acta Crystallogr. A* 2008, **64**, 112–122.
- ³ L. J. Farrugia, *J. Appl. Crystallogr.* 1999, **32**, 837–838.
- ⁴ C. Ducloiset, P. Jouin, E. Paredes, R. Guillot, M. Sircoglou, M. Orio, W. Leibl and A. Aukauloo, *Eur. J. Inorg. Chem.*, 2015, 5405.
- ⁵ J. G. Sharefkin, H. Saltzman, *Org. Synth.* 1963, **43**, 60.
- ⁶ M. R. Mills, A. C. Weitz, M. P. Hendrich, A. D. Ryabov, T. J. Collins, *J. Am. Chem. Soc.* 2016, **138**, 13866.
- ⁷ Similarly broad and ill-defined signals were observed with parent dipyrin iron complexes : C. Kleinlein, S. L. Zheng, T. A. Betley, *Inorg. Chem.*, 2017, **56**, 5892.
- ⁸ Gaussian 09, Revision D.01, M. J. Frisch, G. W. Trucks, H. B. Schlegel, G. E. Scuseria, M. A. Robb, J. R. Cheeseman, G. Scalmani, V. Barone, B. Mennucci, G. A. Petersson, H. Nakatsuji, M. Caricato, X. Li, H. P. Hratchian, A. F. Izmaylov, J. Bloino, G. Zheng, J. L. Sonnenberg, M. Hada, M. Ehara, K. Toyota, R. Fukuda, J. Hasegawa, M. Ishida, T. Nakajima, Y. Honda, O. Kitao, H. Nakai, T. Vreven, J. A. Montgomery, Jr., J. E. Peralta, F. Ogliaro, M. Bearpark, J. J. Heyd, E. Brothers, K. N. Kudin, V. N. Staroverov, T. Keith, R. Kobayashi, J. Normand, K. Raghavachari, A. Rendell, J. C. Burant, S. S. Iyengar, J. Tomasi, M. Cossi, N. Rega, J. M. Millam, M. Klene, J. E. Knox, J. B. Cross, V. Bakken, C. Adamo, J. Jaramillo, R. Gomperts, R. E. Stratmann, O. Yazyev, A. J. Austin, R. Cammi, C. Pomelli, J. W. Ochterski, R. L. Martin, K. Morokuma, V. G. Zakrzewski, G. A. Voth, P. Salvador, J. J. Dannenberg, S. Dapprich, A. D. Daniels, O. Farkas, J. B. Foresman, J. V. Ortiz, J. Ciosowski, and D. J. Fox, Gaussian, Inc., Wallingford CT, 2013.
- ⁹ a) A. D. Becke, *J. Chem. Phys.* 1993, **98**, 5648–5652.; b) C. Lee, W. Yang, R. G. Parr, *Phys. Rev. B* 1988, **37**, 785–789.
- ¹⁰ A) M. Katari, E. Nicol, V. Steinmetz, G. van der Rest, D. Carmichael, G. Frison, *Chem. Eur. J.* 2017, **23**, 8414–8423; b) E. Andris, R. Navrátil, J. Jašík, T. Terencio, M. Srnec, M. Costas, J. Roithová, *J. Am. Chem. Soc.* 2017, **139**, 2757–2765 and references herein.
- ¹¹ A. Schaefer, C. Huber, and R. Ahlrichs, *J. Chem. Phys.*, 1994, **100**, 5829-35
- ¹² F. Weigend and R. Ahlrichs, *Phys. Chem. Chem. Phys.*, 2005, **7**, 3297-305